


SCIENTIFIC ARTICLE

Biomechanical Effect of C₅/C₆ Intervertebral Reconstructive Height on Adjacent Segments in Anterior Cervical Discectomy and Fusion - A Finite Element Analysis

Jia-ming Zhou, MD^{1,2†}, Xing Guo, MD^{1,2†}, Liang Kang, MD^{1,2†}, Rui Zhao, MD^{1,2}, Xiao-tian Yang, MD^{1,2}, Yi-bin Fu, PhD³, Yuan Xue, MD, PhD^{1,2} 

¹Department of Orthopaedic Surgery and ²Tianjin Key Laboratory of Spine and Spinal Cord, Tianjin Medical University General Hospital, Tianjin, China and ³School of Computing and Mathematics, Keele University, Keele, UK

Objective: To investigate the biomechanical effect of different intervertebral reconstructive heights on adjacent segments following C₅/C₆ anterior cervical discectomy and fusion (ACDF) through finite element analysis.

Methods: A finite element model of intact C₄-C₇ segments was developed and validated for the present study. Five additional C₄-C₇ postoperative models were constructed with 100%, 125%, 150%, 175%, and 200% of the benchmark height of C₅/C₆ on the basis of the intact model. The changes in intradiscal pressure (IDP) and range of motion (ROM) of adjacent segments before and after reconstruction of C₅/C₆ were analyzed.

Results: For the upper adjacent segment (C₄/C₅), the IDPs under the different loading conditions all increased after reconstruction. The maximum IDPs were 0.387, 0.489, 0.491, and 0.472 MPa under flexion, extension, axial rotation, and lateral bending, respectively, observed at the reconstructive height of 200%. The minimum IDPs were observed at 150% reconstructive height under all loading conditions except extension, and were 57, 86 and 81% of the maximum IDPs under flexion, axial rotation, and lateral bending, respectively. The minimum IDP under extension occurred when the reconstructive height is 125% of the benchmark height. For the lower adjacent segment (C₆/C₇), the IDPs of postoperative models under all loading conditions also increased compared to the preoperative model. The maximum IDPs after reconstruction under flexion, extension, axial rotation, and lateral bending were 0.402, 0.411, 0.461, and 0.497 MPa, respectively, when the height of the reconstruction was 200% of the benchmark. The minimum IDPs were observed after a reconstruction at 150% of the benchmark, and were 59%, 85%, 82%, and 81% of the maximum IDPs under flexion, extension, axial rotation, and lateral bending loading conditions.

Conclusions: The reconstructive height is an important factor affecting the IDP and the ROM of adjacent segments after ACDF. To delay the adjacent segment disease, an intervertebral reconstructive height of 150% is an appropriate height in C₅/C₆ ACDF.

Key words: Adjacent segment disease; Anterior cervical discectomy and fusion; Finite element analysis; Intervertebral reconstructive height

Address for correspondence Yuan Xue, MD, PhD, Department of Orthopaedic Surgery, Tianjin Medical University General Hospital, Heping District, Tianjin, China 300052 Tel: +86-22-60814688; Fax: +86-22-27219052; Email: xueyuanzyy@163.com

[†]These authors contributed equally to this work.

Disclosure: The authors declare that they have no conflict of interest.

Received 7 November 2020; accepted 16 March 2021

Introduction

Cervical degenerative disc disease is arguably the most common pathology of the cervical spine, mainly including cervical radiculopathy, cervical myelopathy, and a combination¹. Cervical radiculopathy is pain in unilateral or bilateral upper extremities, often in the setting of neck pain, secondary to compression or irritation of nerve roots in the cervical spine. Cervical myelopathy is a degenerative change in the vertebral column that results in symptoms of a spinal cord disorder that range from dexterity or balance disturbances to quadriplegia and incontinence². In addition, cervical myelopathy patients may also complain of atypical symptoms, including vertigo, blurred vision, nausea, and hypomnesia^{3,4}. For patients unresponsive to appropriate nonsurgical measures for at least 6 months, surgical treatment should be considered⁵. Primary aims of surgery are to relieve radiating arm pain in case of radiculopathy and to prevent progression of neurological deficit in case of myelopathy.

First introduced by Smith and Robinson, anterior cervical discectomy and fusion (ACDF) is currently the gold standard surgical treatment for affected patients^{6–8}. ACDF can achieve stabilization and solid arthrodesis with good clinical outcomes and lower complications. However, many studies have found that cervical fusion can lead to the degeneration of adjacent segments, eventually result in adjacent segment disease (ASD)^{9–11}. ASD is defined as a new clinical finding that corresponds to radiographic signs of the degeneration of adjacent segments. As a complication of ACDF, ASD has led to 5.6% of ACDF patients having to undergo a second surgery, which significantly increases the economic burden on society¹².

There have been a few studies suggested that intervertebral reconstructive height^{13,14}, plate-to-disc distance⁹, and post-operative segmental alignment¹⁵ are factors that affect the incidence of ASD. Chung *et al.*⁹ reviewed 177 patients who underwent ACDF using cervical plates, with follow-up periods of at least 10 years. In this study, they found most clinical adjacent-segment degeneration appeared on the patients with a plate-to-disc distance less than 5 mm. Hence, they considered that to prevent ASD, the plate-to-disc distance should be 5mm or more if possible. Katsuura *et al.*¹⁵ found that for patients with ACDF, postoperative kyphotic change in the fused segment is a factor of ASD.

In addition, reconstructive height is considered to be an important factor affecting the development of ASD. However, the most suitable reconstructive height is controversial. Smith and Robinson⁸ indicated that the 10–15 mm reconstructive height is suitable. White and Panjabi¹⁶ proposed that the intervertebral space should be 4–5 mm. Olsewski *et al.*¹⁷ concluded that the stress significantly decreased when the reconstructive height was in excess of 3 mm. Kawakami *et al.*¹⁸ concluded that 2–5 mm reconstruction is an appropriate reconstructive height, with a lower rate of axial neck pain. Li *et al.*¹³ reported that excessive disc space distraction is a risk factor for the development of radiographic ASD.

Finite element analysis (FEA) has been widely used to investigate the external changes, as well as analyze the internal status of the structural components quantitatively^{19,20}. Through FEA, Sun *et al.*²¹ found that noncontinuous cervical disc arthroplasty could preserve intradiscal pressure (IDP) and facet joint forces at the adjacent and intermediate levels. Ren *et al.*²² found the cervical vertebrae after percutaneous posterior endoscopic cervical discectomy showed good biomechanical performance and stability. Although some scholars have used FEA to calculate the stress state of adjacent segments after ACDF^{22–24}, quantitative analyses of the influence of different reconstructive heights on adjacent segment mechanic bearing by FEA have not been reported. Hence, the objective of the present study was to gain a better understanding of the ASD after ACDF by quantitatively analyzing the effect of different reconstructive heights of C₅/C₆ on the IDP and the cervical vertebrae range of motion (ROM) of adjacent segments after ACDF by FEA.

Material and Methods

Preoperative Model Construction

To establish a finite element (FE) model, we selected a 27-year-old healthy male who had no history of cervical disc disease. We performed a computed tomography (CT) scan of his spine and imported the images into the MIMICS 21.0 (Materialise, Leuven, Belgium) modeling program to obtain the preliminary C₄–C₇ vertebral model. The preliminary model was then smoothed and corrected in Geomagic Studio 14.0 (Geomagic, Research Triangle Park, NC, USA).

Other anatomical structures such as intervertebral disc and cartilage were built using Solidworks 2019 (Solidworks, Waltham, MA, USA). The intervertebral disc is composed of nucleus pulposus, annulus fibers and annulus ground substance. We constructed annulus fibers surrounded the ground substance with an inclination to the transverse plane between 15° and 45°, accounting for approximately 19% of the entire annulus fibrosus volume⁴ in Hypermesh 14.0 (Altair, Troy, MI, USA).

Five groups of ligaments, including the anterior longitudinal ligament (ALL), posterior longitudinal ligament (PLL), ligamentum flavum, interspinous ligament and capsular ligament were established using tension-only spring elements and attached to the corresponding vertebrae. Then, the geometry was imported into Abaqus 6.13 (Simulia Inc., Providence, RI, USA) to set the loading and boundary conditions and output the IDP.

The bony structures of the complete model consisted of the cortical bone, the cancellous bone and the posterior bony elements. The 1.5 mm-thick shell was separated from each cervical vertebra to act as the cortical bone. The 0.2 mm-thick endplates were inserted on the upper and lower sides of the intervertebral discs. The cartilages were inserted into the spaces of the bony articular process joints. All cartilages of the articular processes were subjected to a

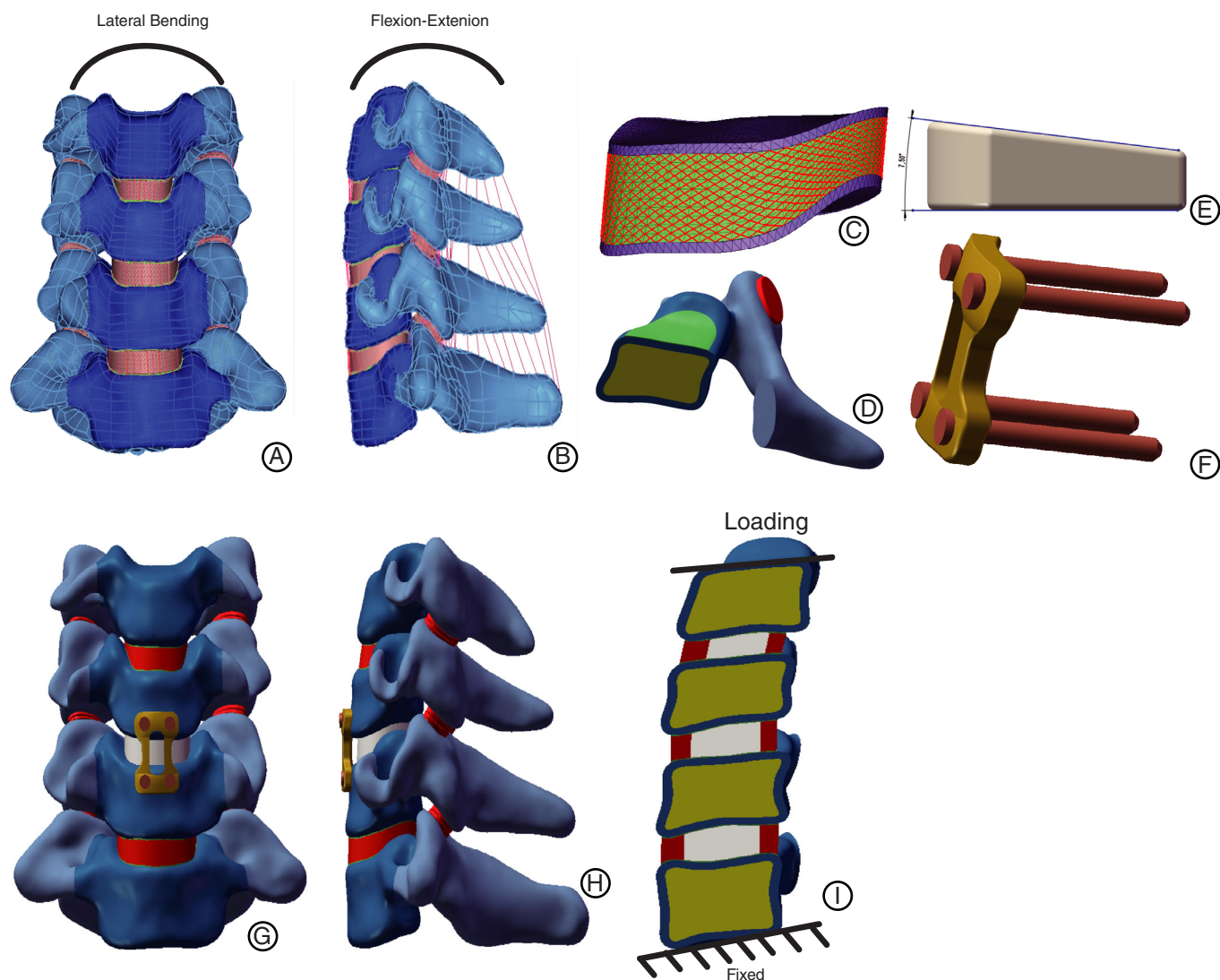


Fig. 1 Finite element models of preoperative and postoperative C₄-C₇ cervical spine and other structures and details. (A) Frontal view of preoperative model; (B) Lateral view of preoperative model; (C) Intervertebral disc details; (D) Vertebral body details; (E) Lateral view of the cage; (F) Titanium plate and screws; (G) Frontal view of postoperative model; (H) Lateral view of postoperative model; (I) Loading and boundary condition.

TABLE 1 The material properties of the spinal soft tissues and hard tissues used in the finite element model

Description	Element type	Young's modulus (MPa)	Poisson's ratio
Cortical bone	C3D4	12,000	0.3
Cancellous bone	C3D4	100	0.2
Posterior elements	C3D4	3500	0.25
Facet cartilage	C3D4	10.4	0.4
End plate	C3D4	600	0.3
Nucleus pulposus	C3D4	1	0.49
Annulus ground substance	C3D4	3.4	0.4
Annulus fibers	T3D2	450	0.45
Titanium plate	C3D4	120,000	0.3
Titanium screw	C3D4	120,000	0.3

nonlinear face-to-face frictionless contact with each other^{25,26}.

Finally, the whole preoperative C₄-C₇ FE model was constructed as shown in Fig. 1. The entire FE model consists of 139,672 solid elements and 299,408 nodes. The material properties are listed in Tables 1 and 2^{27,28}.

Mesh Convergence Test

The FE model was tested for mesh convergence. Three mesh resolutions were generated consecutively (in the order of Mesh 1, Mesh 2, and Mesh 3) for this FE model. Mesh 1 had the smallest number of elements and nodes among the three mesh resolutions. Mesh 2 and Mesh 3 had approximately doubled numbers of elements and nodes than the previous

TABLE 2 The material properties of the ligaments

ALL		PLL		LF		ISL		CL	
Displacement (mm)	Force (N)	Displacement (mm)	Force (N)	Displacement (mm)	Force (N)	Displacement (mm)	Force (N)	Displacement (mm)	Force (N)
0	0	0	0	0	0	0	0	0	0
1	35.5	0.9	1.33	1.7	2.2	1.2	0.75	1.7	2.452
2	64.9	2	29.0	3.74	45.9	2.7	16.9	3.9	53.6
4	89.7	3	51.4	5.61	82.9	4.0	24.4	5.8	87.9
5	108.6	4	71.38	7.48	119.6	5.4	29.5	7.7	109.4
6	119.6	5	85.8	9.35	133.7	6.7	32.9	9.7	125.8
		6	94.7	11.3	147.2	8.1	34.9	11.5	134.8

ALL, anterior longitudinal ligament; CL, capsular ligament; ISL, interspinous ligament; LF, ligamentum flavum; PLL, posterior longitudinal ligament.

TABLE 3 Element and node numbers for three different mesh resolutions

	Element number	Node number
Mesh 1	63218	148526
Mesh 2	139672	299408
Mesh 3	232536	452768

mesh resolution. The number of elements and nodes for each mesh resolution are shown in Table 3. The three mesh resolutions were tested under the same rotation with a moment of 1.0 N·m. The von Mises stress was calculated and compared for different structures in the FE model. When the prediction results obtained by two consecutive mesh resolutions have differences smaller than 5%, the mesh was considered to be convergent^{29,30}.

Validation of the Model

Range of motion of the preoperative C₄-C₇ finite element (FE) model was predicted with a pure bending moment of 1 N·m for flexion, extension, axial rotation, and lateral bending with 73.6 N of axial compression superior to C₄ and compared to previous experimental results³¹. To measure the ROM, we established a cross coordinate system on the superior plane of the target vertebral body, and then measured the ROM in different directions according to the changes in the position of the coordinate system after loading.

Postoperative Models Reconstruction

Generally, during a real procedure, the C₅/C₆ anterior longitudinal ligament, C₅/C₆ disc, inferior endplate of C₅, superior endplate of C₆ and C₅/C₆ posterior longitudinal ligament were resected. Hence, we deleted corresponding structures to simulate the surgery more precisely. In order to reduce the impact of individual differences in the height of the intervertebral discs, we chose the heights of 100%, 125%, 150%, 175%, and 200% of the benchmark height.

In addition, because cervical disc degeneration mostly occurs in the C₅/C₆ segment, we selected the C₅/C₆ segment for the simulation of the surgical segment so that the results could be suitable for more patients. The preoperative C₅/C₆ intervertebral height was 5.0 mm. Hence, five postoperative FE models were built with heights of 5, 6.25, 7.5, 8.75, and 10 mm at 100%, 125%, 150%, 175% and 200% of the benchmark height.

In the actual operation, the interbody fusion cage (Medtronic Sofamor Danek, Memphis, TN, USA) can increase cervical lordosis of 7.5°, so we simulated the reconstruction to increase the cervical lordosis by 7.5° in all postoperative models. All postoperative models were based on a validated model of the aforementioned preoperative C₄-C₇ model. One of the postoperative models was shown in Fig. 1.

In the present study, the C₅/C₆ anterior titanium alloy plate and self-tapping screws (Medtronic Sofamor Danek, Memphis, TN, USA) were simulated. The length of the titanium alloy plate increases in response to an increase in the reconstructive height, so as to make the screws fixed in the same position of the vertebral body in all postoperative models. The five postoperative models were loaded in flexion, extension, axial rotation, and lateral bending, by imposing a pure moment of 1.0 Nm on C₄ with 73.6 N of axial precompression superior to the upper endplate of C₄. The lower endplate of C₇ was firmly fixed in all degrees of freedom. All related connections were set to binding except the mutual contact between the cartilages of the articular processes.

Results

Mesh Convergence Test

The percentage differences in von Mises stress of Mesh 1 vs. Mesh 2 and Mesh 2 vs. Mesh 3 are shown in Fig. 2. The differences of von Mises stress between Mesh 2 and Mesh 3 were less than 5% in the model. Hence, Mesh 2 was considered to be stress-converged and was chosen for this study.

FE Model Validation

To validate the FE model, we compared the predicted ROMs of our model with the data of previous specimen experiment³¹ under different loading conditions by linear regression analysis. The regression equation and correlation coefficient were obtained as follows: $y = 1.014x - 0.089$, $R^2 = 0.766$. The y-axis represents the ROMs of the FE model and the x-axis represents the ROMs of previous specimen experiment under different loading conditions. The R^2 represents the correlation coefficient of the regression equation, which indicated that the results of the FE model had a correlation with the previous experimental results.

Meanwhile, the comparisons between in vitro data and predicted values in the FE models are shown in Fig. 3. All

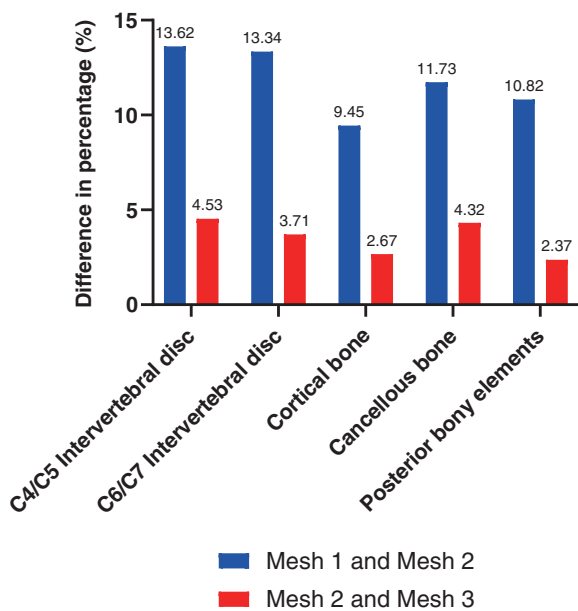


Fig. 2 The predicted percentage differences of von Mises stress between Mesh 1 and Mesh 2 and between Mesh 2 and Mesh 3 in different structures in the axial rotation.

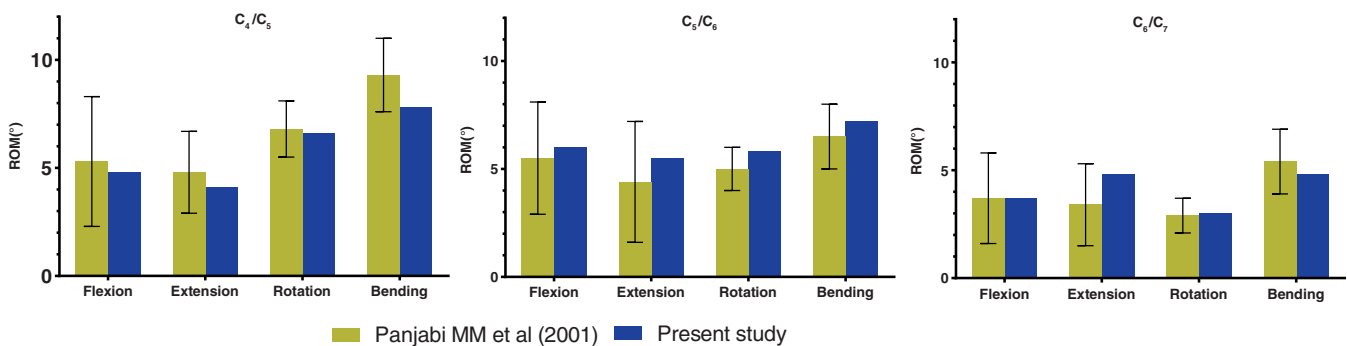


Fig. 3 The predicted ranges of motion (ROM) of the preoperative model are validated by previous published study.

the predicted data in this study occurred within the standard deviation of the mean values of the previous literature³¹, meaning the data was in a good agreement with published experimental results.

Hence, the FE model can be regarded as validated and could be used in the present study.

Adjacent IDPs

The maximum von Mises stresses in upper adjacent segment (C_4/C_5) are shown in Figs 4A and 5 and Table 4. After reconstruction, the adjacent IDPs under the different loading conditions all increased. The maximum adjacent IDPs were 0.387, 0.489, 0.491, and 0.472 MPa under flexion, extension, axial rotation, and lateral bending, respectively, observed at the reconstructive height of 200%. The minimum IDPs were observed after a reconstruction at 150% of the benchmark under all loading conditions except extension, and were 57, 86 and 81% of the maximum IDPs under flexion, axial rotation, and lateral bending, respectively. The minimum IDP under extension occurred when the reconstructive height is 125% of the benchmark height.

The maximum von Mises stresses in lower adjacent segment (C_6/C_7) are shown in Figs 4B and 6 and Table 5. The IDPs of postoperative models under all loading conditions also increased compared to the preoperative model. The maximum IDPs after reconstruction under flexion, extension, axial rotation, and lateral bending were 0.402, 0.411, 0.461, and 0.497 MPa respectively, when the height of the reconstruction was 200% of the benchmark. The minimum IDPs were observed after a reconstruction at 150% of the benchmark, and were 59%, 85%, 82%, and 81% of the maximum IDPs under flexion, extension, axial rotation, and lateral bending loading conditions.

Segmental Motion of Adjacent Levels

The results of the ROM of upper adjacent segment (C_4/C_5) are shown in Fig. 7 and Table 6. After the reconstruction, the ROMs all increased under the four loading conditions. The lowest ROM was found at the 150% reconstructive

height under different loading conditions except extension among the five postoperative models.

The results of the ROM of the lower adjacent segment (C_6/C_7) were shown in Fig. 8 and Table 7. Similarly, the ROM of C_6/C_7 was lowest at the reconstructive height of 150% under all loading conditions among the five postoperative models.

For the fusion segment ($C_{5/6}$), the ROM was significantly reduced and approached 0° in all loading conditions.

Discussion

Controversy in Reconstructive Height

ACDF is currently the gold standard surgical treatment for affected patients. However, many studies^{11,32} have reported that ACDF can accelerate the degeneration of adjacent segments, but the specific mechanism is still not very clear.

The reconstructive height is considered to be an important factor affecting the development of ASD. Lack of distraction may cause insufficient decompression or cervical

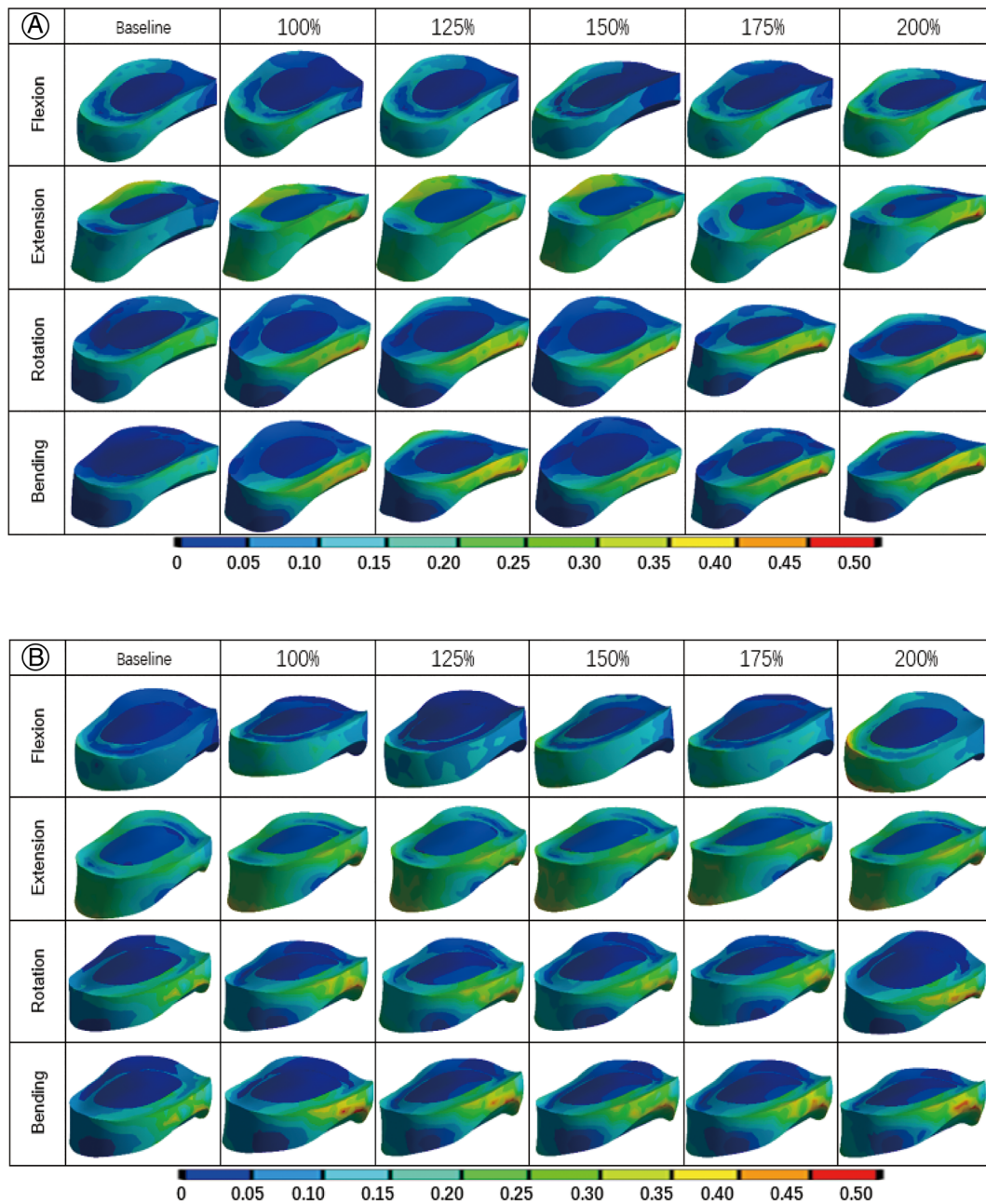


Fig. 4 The intradiscal pressures distribution diagram of adjacent intervertebral discs. (A) C_4/C_5 ; (B) C_6/C_7 .

TABLE 4 The maximum von Mises stress (MPa) in C₄/C₅ segment under different loading conditions

	Baseline	100%	125%	150%	175%	200%
Flexion	0.208	0.242	0.236	0.221	0.307	0.387
Extension	0.313	0.383	0.327	0.340	0.467	0.489
Rotate	0.253	0.463	0.435	0.423	0.459	0.491
Lateral bending	0.272	0.469	0.460	0.384	0.455	0.472

TABLE 5 The maximum von Mises stress (MPa) in C₆/C₇ segment under different loading conditions

	Baseline	100%	125%	150%	175%	200%
Flexion	0.215	0.289	0.283	0.239	0.275	0.402
Extension	0.263	0.393	0.372	0.351	0.369	0.411
Rotate	0.352	0.427	0.403	0.379	0.386	0.461
Lateral bending	0.363	0.483	0.475	0.401	0.479	0.497

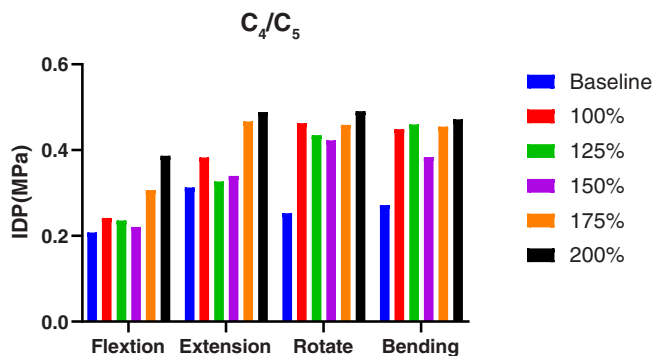


Fig. 5 The intradiscal pressure (IDP) of C₄/C₅ levels under different loading conditions.

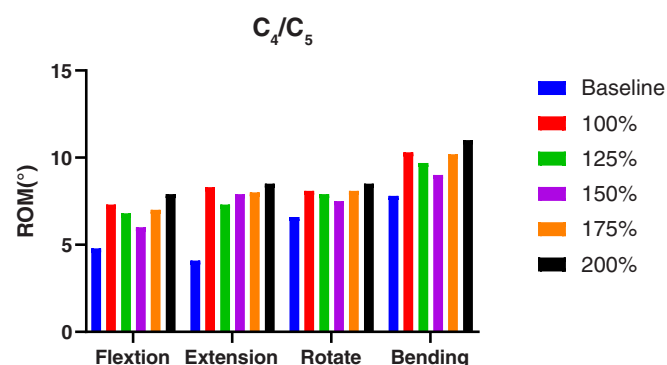


Fig. 7 The range of motion (ROM) of C₄/C₅ levels under different loading conditions.

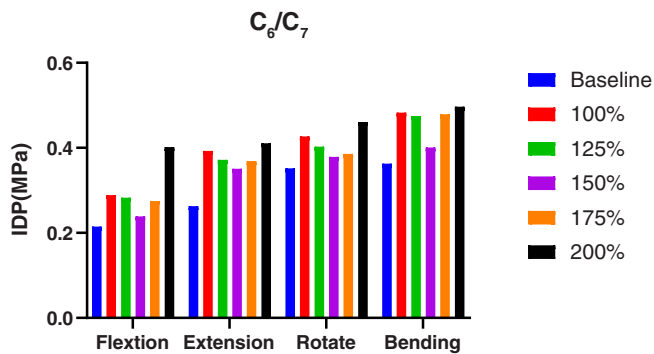


Fig. 6 The intradiscal pressure (IDP) of C₆/C₇ levels under different loading conditions.

TABLE 6 The ROM (°) in C₄/C₅ segment under different loading conditions

	Baseline	100%	125%	150%	175%	200%
Flexion	4.8	7.3	6.8	6.0	7.0	7.9
Extension	4.1	8.3	7.3	7.9	8.0	8.5
Rotate	6.6	8.1	7.9	7.5	8.1	8.5
Lateral bending	7.8	10.3	9.7	9.0	10.2	11.0

ROM, range of motion.

kyphosis. However, excessive distraction may lead to increased mechanical stress on adjacent segments, eventually resulting in ASD. Hence, the most suitable reconstructive height is still controversial.

Smith and Robinson⁸ indicated that the 10–15 mm reconstructive height is suitable. White and Panjabi¹⁶ proposed that the intervertebral space should be 4–5 mm. Olsewski *et al.*¹⁷ concluded that the stress significantly decreased when the reconstructive height was in excess of 3 mm. Kawakami *et al.*¹⁸ concluded that 2–5 mm reconstruction is an appropriate reconstructive height, with a lower rate of axial neck pain. Li *et al.*¹³ reported that excessive disc space distraction is a risk factor for the development of radiographic ASD.

IDP after Reconstruction

In our study, compared with preoperative results, the IDPs after the fusion all increased. Eck *et al.*³³ found the same result in a cadaveric experiment. Furthermore, lowest IDPs of adjacent segments were found at 150% reconstructive height compared with other models of height except C₄/C₅-extension-condition after ACDP. It has been reported that excessive loading can induce degeneration of intervertebral discs³⁴. Hence, achieving the lower IDP is beneficial to delay the degeneration of the intervertebral disc.

ROM after Reconstruction

In our study, we also found the ROM of the cervical vertebrae for C₄/C₅ and C₆/C₇ both increased after reconstruction.

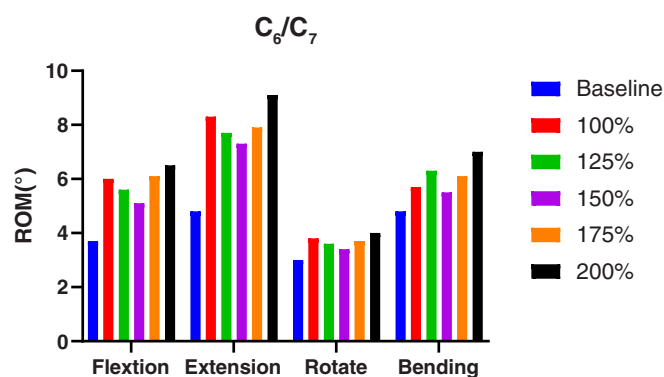


Fig. 8 The range of motion (ROM) of C₆/C₇ levels under different loading conditions.

TABLE 7 The ROM (°) in C₆/C₇ segment under different loading conditions

	Baseline	100%	125%	150%	175%	200%
Flexion	3.7	6	5.6	5.1	6.1	6.5
Extension	4.8	8.3	7.7	7.3	7.9	9.1
Rotate	3	3.8	3.6	3.4	3.7	4
Lateral bending	4.8	5.7	6.3	5.5	6.1	7

ROM, range of motion.

Meanwhile, we found that when the reconstructive height is 150% of benchmark height, the ROM of adjacent segments under all loading conditions except the C₄/C₅-extension-condition were lowest in the five postoperative models. Elsawaf *et al.*³⁵ have reported that the increase in the ROM of the adjacent levels accelerates the degeneration of adjacent segments. Eck *et al.*³³ proposed that adjacent ROM increases at both superior and inferior adjacent segments following C₅/C₆ ACDF during flexion and extension in cadaveric cervical spines and speculated that this increase is related to the incidence of ASD. White and Panjabi³⁶ proposed that as the motion of adjacent vertebral body increases, the risk of

developing ASD increases as well. Therefore, 150% intervertebral reconstructive height has the least influence on the ROM of adjacent cervical vertebrae that is beneficial to delaying the degeneration of adjacent segments.

Considering that the increase in IDP and ROM of adjacent vertebrae can cause the degeneration of the adjacent segments, the intervertebral reconstructive height of 150% is most suitable compared to other heights in C₅-C₆ ACDF, this may serve as a protective factor against ASD.

Limitations

The present study has a number of limitations: (i) the restoration of cervical lordosis by the reconstruction is affected by muscles, surgical technique and many other factors, which should be explored in a further study; (ii) muscles and other soft tissue were not constructed in the models, however, these structures are extremely important for spine biomechanics research; (iii) The screws were designed as solid cylinders bound to the cage or plate, and the threads on the screws were not modeled; (iv) the model was based on only one person, which may limit the present study's applicability to a wider population; and (v) some simplifications were carried out in the prosthesis geometry. For example, we simplify the cancellous bone as a solid structure which may affect the distribution and geometric deformation of the load. Although completely duplicating the result of in vivo studies in FE analysis was impossible, this study effectively shows the biomechanical differences among different intervertebral reconstructive height models.

Conclusion

The reconstructive height is an important factor affecting the IDP and the cervical vertebrae ROM of adjacent segments after ACDF. To delay the degeneration of adjacent segments, an intervertebral reconstructive height of 150% is an appropriate height in C₅/C₆ ACDF.

Acknowledgements

This study was funded by the National Natural Science Foundation of China (Grant No. 81871124) and the Key Program of Tianjin Natural Science Foundation (Grant No. 20JJCZDJC00310).

References

- Adams MA, Roughley PJ. What is intervertebral disc degeneration, and what causes it?. *Spine (Phila Pa 1976)*, 2006, 31: 2151–2161.
- Bernhardt M, Hynes RA, Blume HW, White AA III. Cervical spondylotic myelopathy. *J Bone Joint Surg Am*, 1993, 75: 119–128.
- Chen Z, Wang Q, Liang M, *et al.* Visual cortex neural activity alteration in cervical spondylotic myelopathy patients: a resting-state fMRI study. *Neuroradiology*, 2018, 60: 921–932.
- Chen Z, Zhao R, Wang Q, *et al.* Functional connectivity changes of the visual cortex in the cervical spondylotic myelopathy patients: A resting-state fMRI study. *Spine (Phila Pa 1976)*, 2020, 45: E272–E279.
- Zhou J, Li L, Li T, Xue Y. Preoperative modic changes are related to axial symptoms after anterior cervical discectomy and fusion. *J Pain Res*, 2018, 11: 2617–2623.
- Garvey TA, Eismont FJ. Diagnosis and treatment of cervical radiculopathy and myelopathy. *Orthop Rev*, 1991, 20: 595–603.
- Lin W, Xue Y, Zhao Y, *et al.* Disc associating axial pain were indicated by PLL resection in ACDF surgery. *Eur Spine J*, 2017, 26: 1211–1216.
- Smith GW, Robinson RA. The treatment of certain cervical-spine disorders by anterior removal of the intervertebral disc and interbody fusion. *J Bone Joint Surg Am*, 1958, 40: 607–624.
- Chung JY, Kim SK, Jung ST, Lee KB. Clinical adjacent-segment pathology after anterior cervical discectomy and fusion: results after a minimum of 10-year follow-up. *Spine J*, 2014, 14: 2290–2298.
- Matsumoto M, Okada E, Ichihara D, *et al.* Anterior cervical decompression and fusion accelerates adjacent segment degeneration: comparison with asymptomatic volunteers in a ten-year magnetic resonance imaging follow-up study. *Spine (Phila Pa 1976)*, 2010, 35: 36–43.

11. Wang F, Hou HT, Wang P, Zhang JT, Shen Y. Symptomatic adjacent segment disease after single-lever anterior cervical discectomy and fusion: Incidence and risk factors. *Medicine (Baltimore)*, 2017, 96: e8663.
12. Wu JC, Liu L, Wen-Cheng H, *et al.* The incidence of adjacent segment disease requiring surgery after anterior cervical discectomy and fusion: estimation using an 11-year comprehensive nationwide database in Taiwan. *Neurosurgery*, 2012, 70: 594–601.
13. Li J, Li Y, Kong F, Zhang D, Zhang Y, Shen Y. Adjacent segment degeneration after single-level anterior cervical decompression and fusion: disc space distraction and its impact on clinical outcomes. *J Clin Neurosci*, 2015, 22: 566–569.
14. Xiong W, Zhou J, Sun C, *et al.* 0.5- to 1-Fold intervertebral distraction is a protective factor for adjacent segment degeneration in single-level anterior cervical discectomy and fusion. *Spine (Phila Pa 1976)*, 2020, 45: 96–102.
15. Katsuura A, Hukuda S, Saruhashi Y, Mori K. Kyphotic malalignment after anterior cervical fusion is one of the factors promoting the degenerative process in adjacent intervertebral levels. *Eur Spine J*, 2001, 10: 320–324.
16. White AA III, Panjabi MM. Biomechanical considerations in the surgical management of cervical spondylotic myelopathy. *Spine (Phila Pa 1976)*, 1988, 13: 856–860.
17. Olsewski JM, Garvey TA, Schendel MJ. Biomechanical analysis of facet and graft loading in a Smith-Robinson type cervical spine model. *Spine (Phila Pa 1976)*, 1994, 19: 2540–2544.
18. Kawakami M, Tamaki T, Yoshida M, Hayashi N, Ando M, Yamada H. Axial symptoms and cervical alignments after cervical anterior spinal fusion for patients with cervical myelopathy. *J Spinal Disord*, 1999, 12: 50–56.
19. Yoganandan N, Kumaresan S, Voo L, Pintar FA. Finite element applications in human cervical spine modeling. *Spine (Phila Pa 1976)*, 1996, 21: 1824–1834.
20. Zhao LM, Tian DM, Wei Y, *et al.* Biomechanical analysis of a novel intercalary prosthesis for humeral diaphyseal segmental defect reconstruction. *Orthop Surg*, 2018, 10: 23–31.
21. Sun X, Sun S, Zhang T, Kong C, Wang W, Lu S. Biomechanical comparison of noncontiguous cervical disc arthroplasty and noncontiguous cervical discectomy and fusion in the treatment of noncontinuous cervical degenerative disc disease: a finite element analysis. *J Orthop Surg Res*, 2020, 15: 36.
22. Ren J, Li R, Zhu K, *et al.* Biomechanical comparison of percutaneous posterior endoscopic cervical discectomy and anterior cervical decompression and fusion on the treatment of cervical spondylotic radiculopathy. *J Orthop Surg Res*, 2019, 14: 71.
23. Fernandes PC, Fernandes PR, Folgado JO, Levy MJ. Biomechanical analysis of the anterior cervical fusion. *Comput Methods Biomech Biomed Engin*, 2012, 15: 1337–1346.
24. Maiman DJ, Kumaresan S, Yoganandan N, Pintar FA. Biomechanical effect of anterior cervical spine fusion on adjacent segments. *Biomed Mater Eng*, 1999, 9: 27–38.
25. Denozière G, Ku DN. Biomechanical comparison between fusion of two vertebrae and implantation of an artificial intervertebral disc. *J Biomech*, 2006, 39: 766–775.
26. Rong X, Wang B, Ding C, *et al.* The biomechanical impact of facet tropism on the intervertebral disc and facet joints in the cervical spine. *Spine J*, 2017, 17: 1926–1931.
27. Wheeldon JA, Stemper BD, Yoganandan N, Pintar FA. Validation of a finite element model of the young normal lower cervical spine. *Ann Biomed Eng*, 2008, 36: 1458–1469.
28. Yoganandan N, Kumaresan S, Pintar FA. Biomechanics of the cervical spine Part 2. Cervical spine soft tissue responses and biomechanical modeling. *Clin Biomech (Bristol, Avon)*, 2001, 16: 1–27.
29. Ayturk UM, Puttlitz CM. Parametric convergence sensitivity and validation of a finite element model of the human lumbar spine. *Comput Methods Biomech Biomed Engin*, 2011, 14: 695–705.
30. Jones AC, Wilcox RK. Finite element analysis of the spine: towards a framework of verification, validation and sensitivity analysis. *Med Eng Phys*, 2008, 30: 1287–1304.
31. Panjabi MM, Crisco JJ, Vasavada A, *et al.* Mechanical properties of the human cervical spine as shown by three-dimensional load-displacement curves. *Spine (Phila Pa 1976)*, 2001, 26: 2692–2700.
32. Bydon M, Xu R, Macki M, *et al.* Adjacent segment disease after anterior cervical discectomy and fusion in a large series. *Neurosurgery*, 2014, 74: 139–146 discussion 146.
33. Eck JC, Humphreys SC, Lim TH, *et al.* Biomechanical study on the effect of cervical spine fusion on adjacent-level intradiscal pressure and segmental motion. *Spine (Phila Pa 1976)*, 2002, 27: 2431–2434.
34. Raj PP. Intervertebral disc: anatomy-physiology-pathophysiology-treatment. *Pain Pract*, 2008, 8: 18–44.
35. Elsawaf A, Mastronardi L, Roperto R, Bozzao A, Caroli M, Ferrante L. Effect of cervical dynamics on adjacent segment degeneration after anterior cervical fusion with cages. *Neurosurg Rev*, 2009, 32: 215–224 discussion 224.
36. Panjabi MM, White AA III. Basic biomechanics of the spine. *Neurosurgery*, 1980, 7: 76–93.